Proceedings of the Sixth International Conference on
Railway Technology: Research, Development and Maintenance
Edited by: J. Pombo
Civil-Comp Conferences, Volume 7, Paper 14.8
Civil-Comp Press, Edinburgh, United Kingdom, 2024
ISSN: 2753-3239, doi: 10.4203/ccc.7.14.8

Preliminary Design of a WSP System for an Articulated Freight Wagon

F. Mazzeo, M. Santelia, E. Di Gialleonardo and S. Melzi

Department of Mechanical Engineering, Politecnico di Milano
Italy

Abstract

This study focuses on the implementation of a Wheel Slide Protection (WSP) controller system for an articulated freight wagon. The primary objective of the WSP system is to mitigate wheel sliding on the rail, especially during intense braking manoeuvres under degraded rail conditions. Uncontrolled sliding can lead to severe damage to both the wheels and the infrastructure, posing significant threats to the dynamic stability and overall safety of the entire train.
To address this issue, we develop a comprehensive numerical model of the freight wagon, with a specific emphasis on its pneumatic braking system. Additionally, we incorporate a detailed model of the wheel-rail contact problem, accounting for various rail conditions. Subsequently, we introduce a control logic intended to reduce the wheel sliding and we introduce a physical model of the WSP system to validate the efficacy of the control logic.
This paper presents the outcomes of a preliminary WSP system, showcasing its effectiveness in preventing wheels from sliding. The comprehensive approach taken in modelling and implementing the WSP system contributes valuable insights into enhancing the safety and performance of articulated freight trains, particularly under challenging rail conditions.

Keywords: WSP, articulated freight wagon, pneumatic brake, braking system, wheel-rail contact forces, degraded wheel-rail contact.

1 Introduction

The freight train sector assumes a pivotal role in the logistics system, presenting a significant opportunity to diminish greenhouse gas emissions and noise pollution. The escalating importance of freight trains in the intermodal transportation is highlighted by their capability to exploit the shipping system on rails for extended distances. This approach prioritizes rail transport for the majority of the journey, reserving other transportation methods solely for the critical last mile.

In this framework, a significant amount of work has been done to increase the productivity, safety, and performance of freight trains, e.g. [1],[2]. However, there is still much to be done. Notably, all freight wagons currently lack a Wheel Slide Protection (WSP) system, primarily due to the absence of electronic installations on board these wagons. Given the growing interest in freight rail transportation, there exists the possibility of revamping existing freight wagons. This initiative aims to enhance safety and competitiveness, marking a strategic move towards integrating modern technological solutions into the freight rail sector.

The Wheel Slide Protection (WSP) system is designed to prevent wheel locking during braking maneuvers by dynamically adjusting the braking pressure and reducing the braking torque applied to the wheels. Essentially, when the braking force overcomes a threshold on the wheelset of a railway vehicle—dependent on prevailing wheel-rail conditions—the WSP system intervenes to mitigate and control wheel sliding. The absence of a WSP system increases the risk of wheels undergoing excessive sliding, leading to wheel locking and to the formation of problematic "flat spots" [3]. These, aside from causing stability issues, pose a serious threat to the structural integrity of the rail vehicle, the transported goods, and the rails themselves, generating disruptive vibrations.

Presently, common solutions in the freight sector involve direct wheel replacement after specific mileage or upon detecting irregular wear profiles. An alternative is reprofiling the wheels, a process to restore circular profiles without wheel dismantling. While this option offers material savings compared to direct replacement, it introduces additional constraints and requirements in terms of scheduling, positioning in turning areas, and potential contingencies, resulting in increased labor costs. Recognizing this, the implementation of an active controller emerges as a transformative solution, actively preventing wear processes and increasing the lifetime of the components.

In the context of passenger trains, where electro-pneumatic braking is used, the WSP system is well-known and studied [4],[5],[6]. However, in the field of freight trains, where electronic is notably absent, the WSP system has not received a thorough investigation and for this reason, a detailed model of the vehicle must be developed. In this paper, a significant effort is devoted to the development of the vehicle's model and the pneumatic components of the WSP system. Then, a simple but effective control logic is studied to prove the potential benefits derived from the integration of a WSP system into freight trains. This paper is organized as follows: in section 2 the vehicle model is presented, in section 3 the WSP control logic is described and section 4 reports the results of the analysis.

2 Vehicle Model

The freight wagon (Sdggmrss) is designed for the transport of liftable codified semitrailers and standardized swap containers overall European railway network with normal track gauge. A single wagon has been conceived to run 200.000 km over a single year and is supposed to have a total lifetime total of 20 years; considering the maximum payload achievable (20 tons per axle), the wagon is engineered to reach a maximum speed of 120 km/h.
This wagon consists of two interconnected cars through a Talbot coupling [7], totalling 6 wheelsets and 3 bogies. The braking system of the vehicle is primarily located in the three bogies, each exhibiting some differences, as illustrated in Figure 1.

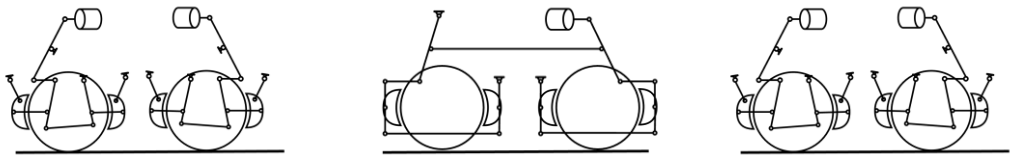

a b c

Figure 1: Scheme of the bogies - 2.a and 2.c extremity bogies. 2.b middle bogie.

At the extremities of the wagon there are two Y25Lssi1-K bogies. They are characterized by a single braking actuator per wheelset, so in total two brake actuators per bogie. Each brake actuator is connected to brake blocks by a rigging system: a set of levers and other components that allow to transfer the relative movement of the single cylinder to all the four brake blocks acting on the wheelset, as shown in Figure 1. In the middle of the wagon there is a Y25Ls(s)1f bogie that has just one brake actuator. This acts on the two wheelsets so the rigging system of the middle bogie is different from the one present in the extremity bogies, as shown in Figure 1.

Pneumatic Layout
The simplified pneumatic layout of the system is represented in Figure *2*. On this vehicle, there are 2 distributors: one is used for one of the extremity bogies, the other is used for the middle and the other extremity bogie. The extremity bogies have 2 brake actuators, while the middle bogie presents a single brake actuator.
It is important to note that the presented scheme serves as a simplified representation of the actual wagon layout. Due to confidentiality reasons, the complete scheme is not disclosed in its entirety; however, this level of detail is not essential for the purpose of this study. Subsequently, the following section provides a description of the general functioning of the brake system.

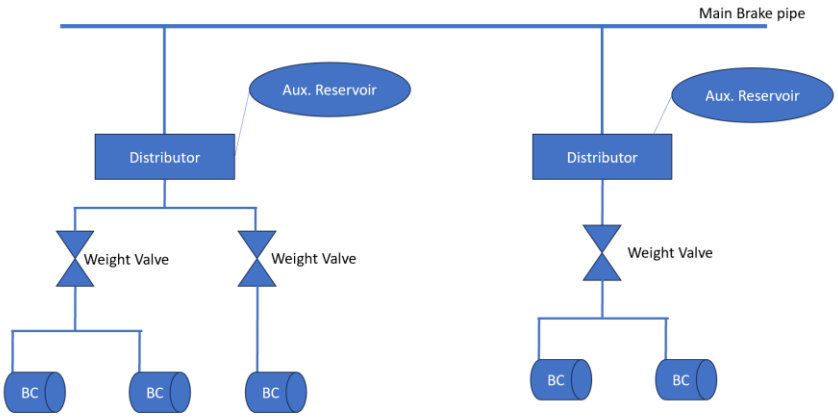

Figure 2: simplified pneumatic scheme of the braking system.

The primary component of the brake system is the Main Brake Pipe (MBP), a pipe interconnected across all wagons, directly connected to the locomotive. In normal operating conditions, the pressure within the MBP is maintained at 5 bar. During braking maneuvers, the driver opens the brake release valve, causing a reduction in MBP pressure that travels through the convoy as a pressure wave [8]. The extent and duration of this pressure reduction depend on the braking maneuver [9]. Connected to the MBP there are distributors, facilitating an increase in pressure within the brake cylinder when a pressure drop occurs in the MBP. Specifically, when the pressure wave reaches a distributor, it generates an increase of the pressure in the braking cylinder based on the MBP's pressure decrease, connecting the auxiliary reservoir (kept at a pressure of 3.6 bar) to the braking cylinder [9]. The maximum pressure achievable within the cylinder is 3.6 bar, reached when the MBP pressure is at 3.5 bar; further reductions in MBP pressure do not affect the maximum pressure in the braking cylinder. Another critical component is the weighting valve, situated between the distributor and the brake cylinder. Functioning as a proportional valve, it modulates the maximum pressure within the brake cylinder based on the wagon's mass. This adjustment is vital as wagons can travel either loaded or empty, and such variations significantly impact braking performance, in accordance with [9].
In particular, in the case of an empty vehicle, the maximum pressure within the braking cylinder is reduced to prevent excessive braking torque, which could lead to wheel locking. Conversely, when the wagon is loaded, the braking pressure in the cylinder reaches its maximum value (3.6 bar) to ensure optimal braking performance, as outlined in [9]. Finally, if there is an intermediate condition between the tare and laden condition, the weighting valve adjusts proportionally the maximum reachable pressure in the cylinder up to 36 t. Each wagon is equipped with three weighting valves (one per bogie) positioned in correspondence with the secondary suspension to modulate the braking characteristics of each bogie.
The characteristic curve of the weight valve is depicted in Figure 3 where the x-axis represents the mass acting on a single bogie, so the sum of the vertical loads acting on the two wheelsets of the bogie. The y-axis illustrates the maximum pressure allowed by the braking valve in the brake actuators.

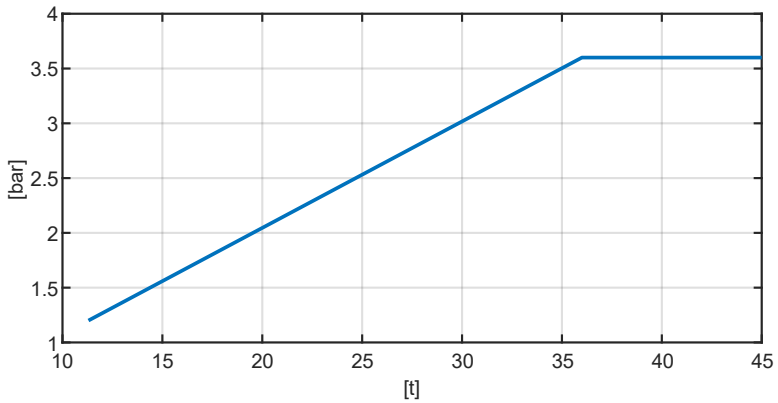

Figure 3: characteristic curve of the weighting valve

Layout of the WSP system

In order to regulate the pressure inside the braking cylinder, WSP valves will be positioned between the weighting valve and the braking cylinder, as illustrated in Figure 4.

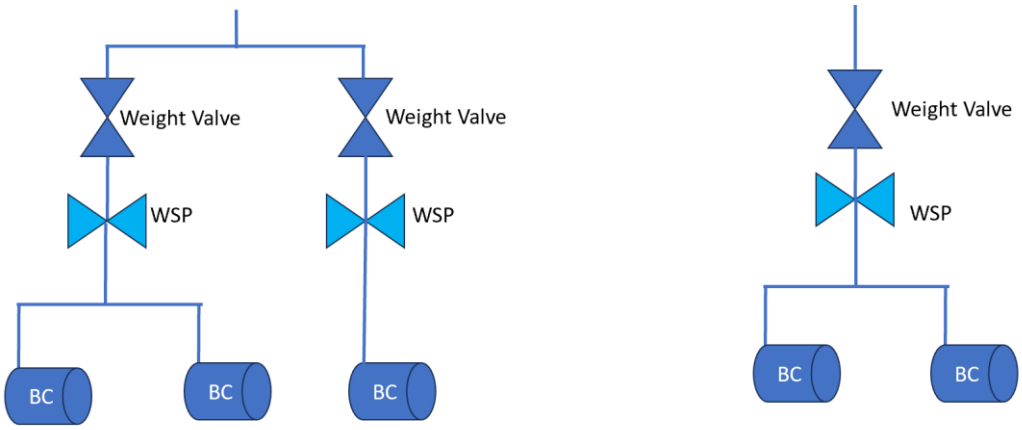

Figure 4: Layout of the WSP system

The chosen configuration employs a single WSP system per bogie, with a total of three WSP systems per wagon, aiming to minimize costs. The WSP operates by measuring the angular speed of the wheelset, as detailed in Section 3. Since the wheelsets are made with fixed wheels, a rotational encoder will be installed on each wheelset, totaling six encoders. The entire system will be controlled by a single electronic board operating at 10 Hz.

While the energy management of the system falls outside the scope of this work, a preliminary scheme could involve a wheel hub generator for energy harvesting and a battery to stabilize the tension.

The pneumatic part of each WSP system is composed of two ON/OFF electro-valves, as shown in Figure *5*.

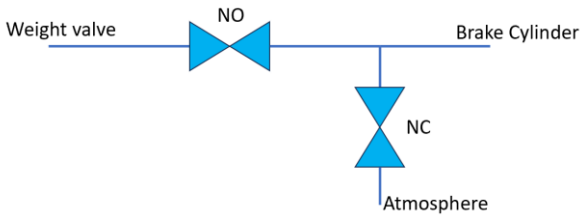

Figure 5: WSP valves arrangement

The component NO in Figure *5* a is normally open, while the NC denotes a normally closed valve. Under regular operating conditions, the valves are not activated, and the system operates in *fill mode*, allowing airflow from the braking system to the brake cylinder. When wheel locking is detected, the WSP system activates, closing NO valve to halt the flow from the brake system and opening NC valve. This configuration is called *release mode*, and it allows air to flow from the braking cylinder to the atmosphere, thereby reducing pressure in the brake cylinder and mitigating braking torque.

Simplified model of the vertical and longitudinal dynamics of the wagon
The vehicle is modelled as a set of rigid bodies in the vertical plane, as represented in Figure *6*.

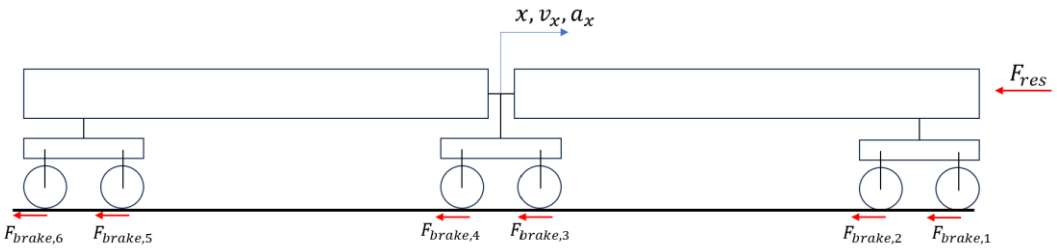

Figure 6: dynamic model of the wagon

In Figure *6* F_{brake} represents the contact brake forces while F_{res} is the resultant of the resistance forces acting on the vehicle. F_{res} is modelled with a quadratic formulation reported in [10]:

$$F_{res} = m(A + Cv^2) \quad (1)$$

Where m is the mass of the vehicle, A and C are constants.
The equilibrium in the longitudinal direction of the system is:

$$\sum F_{brake} + F_{res} = ma_x \quad (2)$$

Finally, the braking forces are obtained considering the rotational equilibrium of each wheel:

$$F_b R - T_b = J\dot{\omega} \tag{3}$$

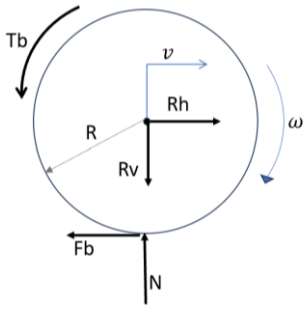

Figure 7: Free-body diagram of the wheel

Considering Figure *7* and equation 3:

- ω is the angular speed of the wheel,
- $\dot{\omega}$ is the angular acceleration of the wheel,
- v is the longitudinal speed of the wheel,
- J is the inertia of the wheel computed around its axis,
- N is the normal contact force acting on each wheel,
- Tb is the braking torque applied on the wheel,
- Fb is the longitudinal contact (braking) force,
- Rh and Rv represent the reaction forces exchanged between the wheel and the bogie in the journal.

The braking torque is computed considering the pressure inside the brake actuator:

$$Tb = i_{tot} P_{brake} \tag{4}$$

The coefficient i_{tot} considers the geometry of the brake actuator, the rigging system, the friction coefficient between the brake pad and wheel, and the geometry of the wheel. This coefficient is assumed to be constant, and its value is obtained from the datasheet of the wagon. The parameter i_{tot} differs slightly between the middle bogie and the extremity one due to variations in their respective rigging systems.
The longitudinal contact force is computed using the Polach model described in [12]. The force is dependent on the longitudinal creepage, defined as:

$$s_x = \frac{v - \omega R}{v} \tag{5}$$

Where v is the longitudinal speed of the wheel, which is equal to the speed of the vehicle. ω is the rotation velocity of the wheel and R is the radius.

The longitudinal contact force can be computed as:

$$F_{brake} = -\frac{2\mu N}{\pi}\left(\frac{K_A\epsilon}{1+(K_A\epsilon)^2} + \text{atan}(k_S\epsilon)\right) \quad (6)$$

$$\epsilon = \frac{1}{4}\frac{G\pi abc_{11}}{N\mu}s_x \quad (7)$$

$$\mu = \mu_0[(1-A)e^{-Bw} + A] \quad (8)$$

$$w = |s_x|v \quad (9)$$

Where μ_0, K_A, K_S, A, B are constants of the Polach model, depending on the rail conditions. The values used in this work are reported in Table 1. In particular, G is the shear module of the steel and a, b are the semi axes of the contact ellipse, according to Hertz theory, and finally c_{11} derives from Kalker theory [13].
An example of the behavior of the longitudinal contact force, with respect to longitudinal velocity and creep ratio, is reported in Figure 8.

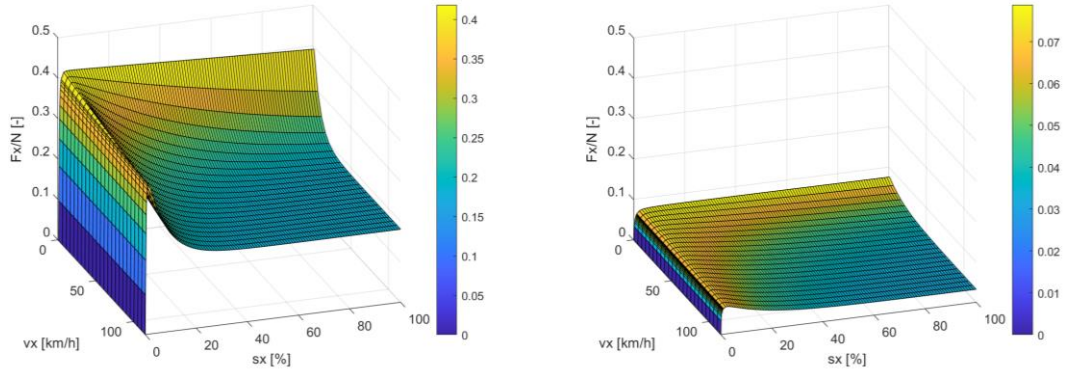

a b

Figure 8: Polach contact model. a: Dry condition; b: Degraded condition.

Parameters	Dry Condition	Degraded condition
μ_0	0.42	0.08
k_A	0.6	0.38
k_S	0.59	0.13
A	0.43	0.4
B	0.42	0.20

Table 1 Parameters used for Polach contact model [6][11]

3 Model of the WSP system

The modeling of the WSP system consists of two parts: the pneumatic model of the valves and the design of the controller.

Pneumatic model of the valves

The flux through each valve is modeled as the flux through a generic orifice, as described by Lee and Kang in [6]. The activation of the electromagnet is represented by a time delay of the first order, represented in Laplace domain as:

$$\frac{\delta_i}{w_i} = \frac{1}{T_v s + 1} \tag{10}$$

with i = {NO, NC}.

In equation (10), T_v is a time constant, characteristic of the valve, and w_i represents the status of the valve where $w_i = 1$ when the electromagnet is activated and $w_i = 0$ in the opposite case.

The cylinder is assumed to be at constant volume, V_{cyl}. However, in the real system, during the initial phase of the braking maneuver, the piston begins to move from its steady position to recover system backlashes, causing an increase in the volume of the brake cylinder. This variation is neglected in this work as the objective is to modulate pressure without disengaging the brake pads from the wheels. The pressure inside the cylinder, P_{cyl} is determined by considering the effects of the NO and NC valves, as detailed in [6].

$$P_{cyl}(t) = \int \frac{\bar{R}_{air} T_0}{V_{cyl}} \left(\dot{m}_{fill}(t) - \dot{m}_{release}(t) \right) dt \tag{11}$$

$$\dot{m}_{fill} = \delta_{NO}(t) \frac{C_{d,NO}\, A_{NO}}{\bar{R}_{air} T_0} P_{wv}(t) \sqrt{P_{wv}(t) - P_{cyl}(t)} \tag{12}$$

$$\dot{m}_{release} = \delta_{NC}(t) \frac{C_{d,NC}\, A_{NC}}{\bar{R}_{air} T_0} P_{cyl}(t) \sqrt{P_{cyl}(t) - P_{atm}} \tag{13}$$

In the previous equations, $\dot{m}_{fill}(t)$ is the mass flow rate entering the cylinder, while $\dot{m}_{release}(t)$ is the mass flow rate released in the atmosphere. T_0 is the reference temperature of the system, assumed constant at $T_0 = 20$ °C, $\bar{R}_{air}$ is the gas constats of the air, A_i is the section of the orifice and $C_{d,i}$ is the flow coefficient of the valves. Finally, P_{wv} is the pressure entering the WSP system, which is regulated by the weight valve and P_{atm} is the atmospheric pressure

Controller

The control logic of the WSP system involves activating a pair of solenoid valves (NO, NC) if one of the wheels of the corresponding bogie experiences a high risk of slippage. To assess the traction state of the wheels, the controller continuously estimates the creepage, for each wheel of the vehicle, defined as follows:

$$s_{x\_est,j} = \lambda_j = \frac{v_{est} - \omega_j R}{v_{est}} \tag{14}$$

Neglecting curving contributions and assuming that the two wheels of the same wheelset have the same radius, the creepage can be assumed equal for both wheels. Thus, with j we indicate the considered wheelset: $j = \{1, \dots, 6\}$.

Given the vector of measured rotational speeds the controller derives the maximum peripheral velocity $v_{max}^{(\omega)}$ similarly to what is done in [5]:

$$v_{max}^{(\omega)}(t) = \max\big(\omega_j(t)\big)R \tag{15}$$

And assigns a value to v_{est}:

$$v_{est}(t) = \begin{cases} v_{max}^{(\omega)}(t) & if\ a_{est}(t) > a_{min} \\ v_{est}(t - \Delta t) + a_{min}\Delta t & if\ a_{est} \leq a_{min} \end{cases} \tag{16}$$

Where $a_{est}(t)$ is:

$$a_{est}(t) = \frac{v_{est}(t) - v_{est}(t - \Delta t)}{\Delta t} \tag{17}$$

With $a_{min} = -1.5\,\frac{m}{s^2}$. This limitation is necessary to prevent the longitudinal speed v_{est} from being incorrectly estimated when all wheels slide simultaneously, leading the controller to fail to detect the loss of traction [5].

Once the creepage λ_j for each j-th wheel is calculated, the controller acts if this value exceeds a variable parameter threshold as indicated in the Table *2*:

v_{est} $\left[\frac{km}{h}\right]$	0 - 12	12 - 30	30 - 70	70 - 120
λ_{ref} [%]	3.5	1.8	1.2	1

Table 2 reference creepages used for WSP system

The dynamic variation of the threshold λ_{ref} has been calibrated manually by the authors to maximize the performance, based on the results of the simulation. It is starting from an optimal value of 1% (according to friction curves) and then progressively increased to prevent the intervention of the control logic in conditions

where adhesion is sufficient to avoid wheel slipping, since the maximum of the curves changes with the speed.
In addition, a deactivation criterion has been added to the control logic, which, according to UIC regulations, involves deactivating the WSP system below a speed of 3 km/h [14].
When the controller detects a sliding, the NO valve is closed, and the NC valve is opened. In this way, the pressure inside the brake cylinder is reduced and so the braking torque. When the estimated creep becomes lower than the reference value, the situation is restored to the original one, with NC close and NO open.

4 Results

In this section, the benefits of the developed WSP system are demonstrated on an articulated freight wagon in fully loaded conditions. Initially, a simulation is conducted with degraded rail conditions reported in Table 1 and without the activation of the WSP. Figure *9* illustrates the results of this simulation, where the black solid line represents the vehicle speed, and the additional lines depict the wheelset peripheral speed multiplied by the wheelset radius.

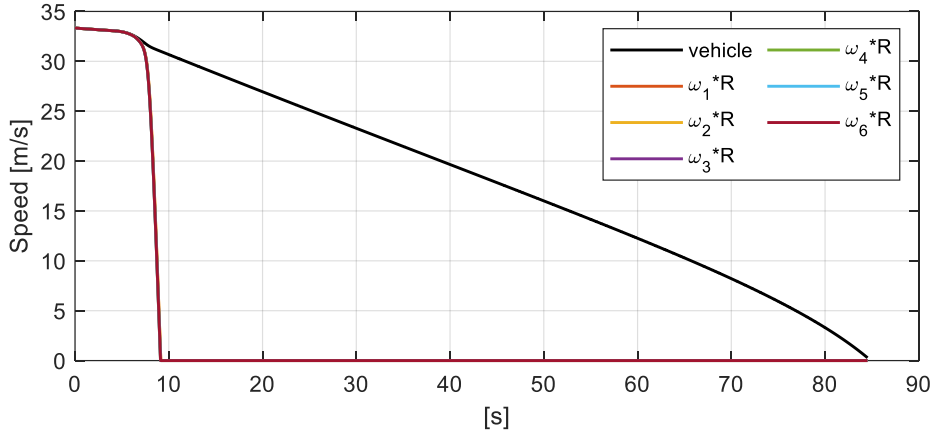

Figure 9: vehicle speed and rotation speed of the wheelset without WSP

It is evident from Figure 9 that the wheels lock immediately at the beginning of the braking phase. In a real maneuver, this scenario could lead to substantial wheel degradation, causing significant wear and the formation of dangerous 'flat spots' [3].
In Figure 10 the same simulation results are presented but considering the activation of the WSP system.
In Figure *10* it is evident that the wheels never fully lock. When the peripheral speed of the wheelset significantly differs from the vehicle speed, the WSP system activates, resulting in a reduction of pressure inside the braking cylinder. This pressure reduction leads to a decrease in braking torque described by equation (4) and effectively prevents wheel locking.
Figure *11* shows the pressure inside the brake cylinders for each bogie, considering the two cylinders of the extremity bogies as one for simplicity. The dashed green

line represents the pressure in the cylinder if the WSP system is not present. On the right y-axis of the same Figure, the status of each WSP system is reported. From Figure *11* it is interesting to notice that the controller acts to modulate the pressure in the braking cylinder, decreasing the mean value.

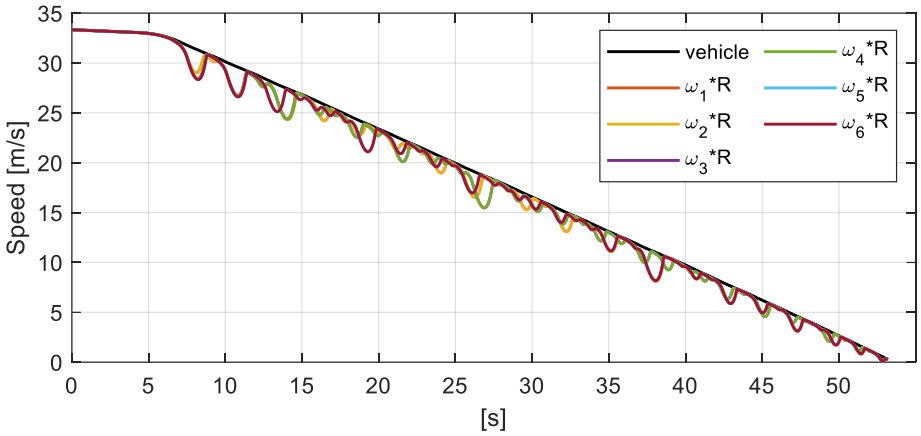

Figure 10: vehicle speed and rotation speed of the wheelset with WSP

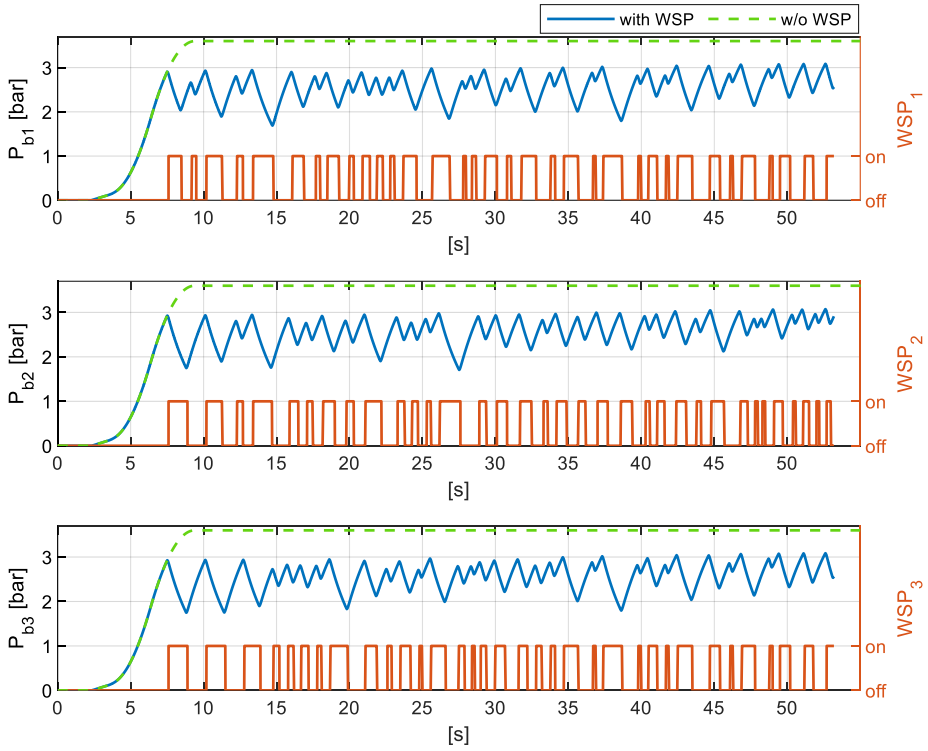

Figure 11: Pressure in the brake cylinders and WSP status. P_{b1} and P_{b3} are the cylinders for the extremity bogies. The two cylinders of the extremity bogies are considered as one for simplicity. P_{b2} is the cylinder of the middle bogie.

In conclusion, Figure *12* illustrates the vehicle acceleration and braking distance during the maneuver, in case of WSP on (solid line) and WSP off (dashed line). It is evident from the figure that, in case of WSP on, the vehicle's deceleration is not constant; instead, it exhibits a certain variability due to the functioning of the WSP system. Moreover, when the WSP is deactivated, the wheels lock and the creepage arrives to 100%. Looking at Figure 8, it is evident that in case of full sliding, the friction coefficient is very low, and this causes a low deceleration of the vehicle with the consequence of long braking distance. Introducing the WSP, is it possible to have a better use of the adhesin forces, limiting the creepage and having a higher friction coefficient with respect to full sliding. This allows reduce the possibility of the formation of flat spots and it reduces the braking distance.

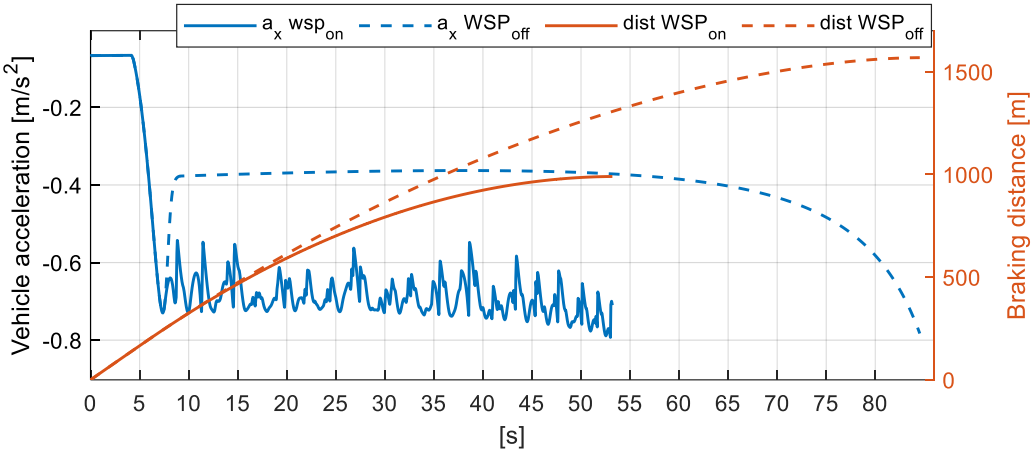

Figure 12: Vehicle acceleration and braking distance in case of WSP on and WSP off.

4 Conclusions

In this paper the model of the braking system of an articulated wagon is analyzed. A pneumatic model of the WSP system is proposed and an effective control strategy is described. The effect of the WSP system is simulated considering the wagon and degraded conditions at wheel-rail interface. The results show the effectiveness of the system in reducing wheel locking.
Although the results presented in this paper appear promising, it is essential to emphasize that the performance in a real-world system may be diminished. This is attributed to the simplifications made in this paper, which aimed to demonstrate the feasibility of the system rather than provide an exhaustive representation of real-world complexities of the systems.

Acknowledgements

This study was carried out within the MOST – Sustainable Mobility National Research Center and received funding from the European Union Next-GenerationEU (PIANO NAZIONALE DI RIPRESA E RESILIENZA (PNRR) – MISSIONE 4

COMPONENTE 2, INVESTIMENTO 1.4 – D.D. 1033 17/06/2022, CN00000023). This manuscript reflects only the authors' views and opinions, neither the European Union nor the European Commission can be considered responsible for them.

References

[1] E. Di Gialleonardo, S. Melzi, and D. Trevisi, "Freight trains for intermodal transportation: optimisation of payload distribution for reducing longitudinal cou-pling forces," Vehicle System Dynamics, pp. 1–19, Sep. 2022, doi: 10.1080/00423114.2022.2120025.

[2] F.Mazzeo, E. Di Gialleonardo, S. Melzi. (2023). An optimal placement of the remote locomotive for minimizing longitudinal coupling forces in freight trains, Proceedings of the 28th IAVSD International Symposium on Dynamics of Vehicles on Roads and Tracks, Ottawa, Canada.

[3] J. Jergéus, C. Odenmarck, R. Lundén, P. Sotkovszki, B. Karlsson, P. Gullsers, Full-scale railway wheel flat experiments, Proc. Inst. Mech. Eng. Part F: J. Rail Rapid Transit. 213 (1) (1999) 1–13. DOI: 10.1243/0954409991530985

[4] G. Barna, "Theoretical analysis of Wheel Slide Protection controllers for rail vehicles," 2011 16th International Conference on Methods & Models in Automation & Robotics, Miedzyzdroje, Poland, 2011, pp. 230-235, doi: 10.1109/MMAR.2011.6031350

[5] L. Pugi, M. Malvezzi , A. Tarasconi , A. Palazzolo , G. Cocci & M. Violani (2 006) HIL simulation of WSP systems on MI-6 test rig, Vehicle System Dynamics, 44:sup1, 843-852, DOI: 10.1080/00423110600886937

[6] Nam-Jin Lee & Chul-Goo Kang (2016) Wheel slide protection control using a command map and Smith predictor for the pneumatic brake system of a railway vehicle, Vehicle System Dynamics, 54:10, 1491-1510, DOI: 10.1080/00423114.2016.1213864

[7] EN 16235:2023. Railway application. Testing for the acceptance of running characteristics of railway vehicles. Freight wagons. Conditions for dispensation of freight wagons with defined characteristics from on-track tests according to EN 14363, 2023

[8] Melzi, S., & Grasso, A. (2018). Development of a numerical model of railway air brake and validation against experimental data. Journal of Advances in Vehicle Engineering, 5(1), 10-17.

[9] UIC 544x01 - Braking Performance. International Union of Railways (UIC)

[10] Rochard BP, Schmid F. A review of methods to measure and calculate train resistances. Proceedings of the Institution of Mechanical Engineers, Part F: Journal of Rail and Rapid Transit. 2000;214(4):185-199. doi:10.1243/0954409001531306

[11] S. Shrestha, M. Spiryagin, Q. Wu, Friction condition characterization for rail vehicle advanced braking system, Mechanical Systems and Signal Processing, Volume 134, 2019, 106324, ISSN 0888-3270, https://doi.org/10.1016/j.ymssp.2019.106324.

[12] O. Polach, Creep forces in simulations of traction vehicles running on adhesion limit, Wear, Volume 258, Issues 7–8, 2005, Pages 992-1000, ISSN 0043-1648,
[13] J.J. Kalker, A fast algorithm for the simplified theory of rolling contact, Vehicle Syst. Dyn. 11 (1982) 1–13.
[14] UIC 544-05: Brakes - Specifications for the construction of various brake parts - Wheel Slide Protection Device (WSP). International Union of Railways (UIC).